AIMS Energy, 13(3): 569–589.
DOI: 10.3934/energy.2025022
Received: 25 March 2025
Revised: 24 May 2025
Accepted: 05 June 2025
Published: 16 June 2025

https://www.aimspress.com/journal/energy

Research article

Optimal operation of flexible IES based on energy hub and demand-side response

Xin Jin[1], Ruoli Tang[2], Tingzhe Pan[1,*], Xin Li[2], Zongyi Wang[1], Chao Jiang[2] and Rui Zhang[2]

[1] Electric Power Research Institute, CSG, Guangzhou 510663, China
[2] School of Naval Architecture, Ocean and Energy Power Engineering, Wuhan University of Technology, Wuhan, Hubei, China

* **Correspondence:** Email: pantz@csg.cn; Tel: +18900220639.

Abstract: In this paper, we explored optimal operation strategies for integrated energy systems (IES) in electrolytic aluminum industrial parks, highlighting energy hubs (EH) as key to improving energy efficiency and operational flexibility. A review of IES research covers system modeling, optimization algorithms, and demand-side response (DR) strategies. By integrating EH into an energy coupling model with a DR framework, we analyzed the system's economic viability, constraints, and optimization approaches. A case study was performed to validate the model's effectiveness across scenarios. Our results demonstrated that the proposed framework significantly improves IES performance: When compared with single-energy-conversion equipment configurations, the EH-integrated model reduces total operating costs by 21.05%–38.02%. By incorporating a DR model tailored to electrolytic aluminum's rigid load characteristics, including load shifting and multi–energy substitution, the system achieves a 53.6%–62.1% reduction in wind/solar curtailment rates and shortens energy storage payback periods by 18.7%. Further analysis indicated that the DR-IES model can dynamically balance electrical and thermal loads, incentivize user participation, and enhance environmental benefits. Empirical results showed that this approach reduces total operating costs by 5.56% and narrows the peak-valley differences of electrical and thermal loads by 24.78% and 17.11%, respectively. This study provides a new paradigm for high-energy-consuming industries to achieve low–carbon transformation through the collaborative optimization of EH and DR, offering theoretical and practical guidance for energy management in industrial parks.

Keywords: integrated energy system; energy hub; demand response; electrolytic aluminum industry; energy utilization efficiency

1. Introduction

With the accelerated global energy transition and the growing diversification of energy demands, the optimization of integrated energy systems (IESs) and the development of demand-side response (DR) strategies have emerged as vital research topics in the energy sector. By integrating multiple energy carriers, including electricity, heat, and gas, IES significantly enhances energy conversion efficiency and fosters synergistic optimization. This integration leads to improved energy efficiency, reduced consumption costs, and increased system flexibility and stability. Scholars worldwide have dedicated extensive research to this field, resulting in a multitude of innovative theories and methodologies.

IESs are effective for building green and low-carbon industrial parks. The energy hubs (EHs) play a pivotal role in the studies on IES. The EH is the key node for energy transmission and conversion, which dictates the processes of energy transformation and distribution. The various modeling methods of EH provide critical theoretical support for the analysis of IESs. They also enable to accurately identify the state of the IES from the perspective of a multidimensional performance indicator. By developing EH models, many evaluation indicators, such as the energy utilization rate, energy unavailability, and carbon emission level, can be comprehensively considered, which supports the scientific decision-making in several aspects, including the IES network architecture, equipment selection, and scheduling operations [1–3].

Dai et al. [4] proposed a multi-EH load-source coordination optimization method that considers the benefits of energy consumption. They highlighted the key role of EH in promoting the consumption of renewable energy, enabling a reduction in the operational cost and enhance the operational benefit of energy systems. Li et al. [5,6] emphasized the central role of EH in the optimal operation of electric thermal grids, especially when taking the variable energy efficiency of the equipment into consideration. They employed piecewise linearization methods and standardized matrix models to accurately capture the changes of the EH equipment efficiency under different operating conditions. In addition, they increased the forecasting accuracy of operational cost for electric thermal grids and provided a novel perspective on wind power accommodation.

In the aspect of DR in IES, Wang et al. [7] proposed an integrated demand response (IDR) optimization method, which maximizes the use of clean energy and ensures the security of the underlying by developing a multi-energy IES model and designing trading strategies. They adjusted user loads using the demand elasticity matrix to promote energy efficiency and economic benefits via price incentives without increasing total energy consumption. Guo et al. [8] developed a DR model on the user side, incorporating the transferable and dispatchable loads. They also developed an optimal operation model for regional IES, while taking the flexible loads and IDR on the user side into consideration. Their experimental results show that the developed method improves energy utilization flexibility and responsiveness and optimizes system operations by considering user participation. This significantly reduces operational costs and enhances overall energy efficiency. Li et al. [9] proposed an economic optimization scheduling method for industrial park IES based on multi-timescale DR. They developed the optimization scheduling models in three timescales: Day-ahead, intraday, and real-

time. Xu et al. [10] proposed an optimization model that combines the centralized and distributed control for industrial park IES. In their study, the DR model, which includes transferable and dispatchable loads, was developed, and a novel optimization operation planning method for regional IES with DR was proposed. Chong et al. [11] proposed an integrated demand response strategy. They used a linear dynamic thermal network model to build a hybrid time-scale optimal scheduling framework, which cuts operational costs effectively. However, this model is at a low level in scheduling and has not been verified in real systems. Duan et al. [12,13] developed an integrated demand response model that combines price-based and substitution demand responses. Its dynamic incentive mechanism can motivate users to participate in demand response, reduce the system's overall cost, and enhance economic efficiency. However, the model does not fully consider the dynamic impact of energy market price fluctuations on scheduling strategies.

For optimal operation models, Wang et al. [14] proposed an optimal design method for park-level IES based on load characteristics. In this method, the equipment utilization rates, payback periods, renewable energy penetration rates, and user-side energy quality indicators were comprehensively considered. Liu et al. [15–18] developed a two-layer optimization model for regional integrated energy systems. This model covers energy production, storage, load, and trading, aiming to optimize system operation. Zhao et al. [19] presented an R-P-D chain for park-level systems. They also built models for flexibility assessment, coupling coordination, and flexibility adaptation, analyzing the system from multiple dimensions. However, these studies may have model assumptions that deviate from reality. They simplify user behavior, making it difficult to accurately reflect actual demand response. In algorithm applications, Xie et al. [20–22] created a multi-regional and multi-energy system model. It includes demand-response alliances and shared energy storage. Using a multi-objective optimization model, it considers system operation costs and environmental impacts. Case analyses confirm the model's and algorithm's effectiveness. Jordehi et al. [23] formulated a stochastic mixed-integer linear programming model. It evaluates the impact of energy hubs, mobile storage, and demand response plans on power system resilience. Sepehrzad et al. [24] applied K-means clustering and a PSO algorithm. They constructed an integrated energy distribution system model that considers energy-market interactions and user participation. This model determines multidimensional scenarios and solves optimization problems.

As discussed, the studies showed that through energy planning and operational strategy design, it is possible to significantly increase the efficiency and economics of energy utilization while reducing the environmental impact. However, to the best of our knowledge, a study on improving the flexibility of IES in industrial park, especially for the high energy consumption target, such as the electrolytic aluminum industry park, does not exist. In this study, the EH model for IES of electrolytic aluminum industry park is developed to improve the flexibility in the IES design, which incorporates DR technologies for maximizing the energy utilization and optimizing the economic benefits.

The energy management and operations in industrial parks are often managed by multiple independent operators, which results in insufficient information sharing, difficulty in effectively responding to peak demand, low energy utilization efficiency, and waste. The energy demands of industrial parks are diverse and dispersed, which makes the demand-side management the core of the IES operations. An effective DR can enhance the system economics and reduce the user energy costs. Therefore, we analyze the current situation, establish an IES architecture, and clarify the connections between energy types and entities, enabling us to perform efficient energy utilization and cost reduction. An IES that integrates multiple resource supplies and scheduling is introduced. It performs new energy

absorption and DR of the IES, optimizes energy consumption plans, enhances system optimization levels, and reduces user energy costs.

The contributions of this paper are summarized as follows:

(1) A novel IES optimization model, centered around the EH and incorporating comprehensive DR strategies, is developed. This model achieves a balance between electrical and thermal loads through the EH, and incorporates incentives for user participation and environmental benefits, enabling us to significantly increase the flexibility and reliability of the system.

(2) An energy coupling model that leverages the EH as the nucleus is developed. This provides a detailed analysis of the transformation and coupling relationships between different energy forms within the industrial park IES. This yields insights into the economic viability, operational constraints, and optimization strategies of the system, where the EH plays a crucial role.

(3) Data from an industrial park in southern China are employed to conduct a case study analysis. The results validate the effectiveness of the proposed optimization model that is anchored on the EH. They demonstrate that the method reduces operational costs, minimizes wind and solar energy abandonment, and shortens the payback period for energy storage systems, providing practical guidance for optimizing IES operations in industrial parks, considering the EH as a key component.

The remainder of this paper is organized as follows. In Section 2, we outline the basic structure of the IES, then model it, and finally propose an IES model that incorporates IDR. In Section 3, we present the economic model and solution method of the IES. In Section 4, we provide experiments and analysis to validate the proposed model. In Section 5, we conclude the paper with a summary of the findings and suggestions for future work.

2. Industrial park (EH) model

2.1. EH structure

The basic structure of industrial park EH studied in this paper is shown in Figure 1. As shown in the figure, the EH comprises wind turbines (WTs), photovoltaic arrays (PVs), gas turbines (GTs), and waste heat boilers (WHBs) that form combined heating and power (CHP) units, electric boilers (EBs), gas-fired boilers (GBs), electrical energy storage (EES), and heat energy storage (HES).

This industrial park EH can perform energy production, transmission, conversion, and consumption. It also connects power grid companies, gas grid companies, and user loads, enabling us to meet user energy demands through the multi-energy coupling devices of the underlying system. In addition, end-users have electricity and heat demands. The electricity demands are met by WT, PV, CHP, purchased power, and EES, while the heat demands are met by CHP, GB, EB, and HES. EES and HES are crucial ES devices in the system, leveraging the differences in peak and valley times to coordinate and optimize system operations according to the demand, which enables us to increase the energy efficiency of the system.

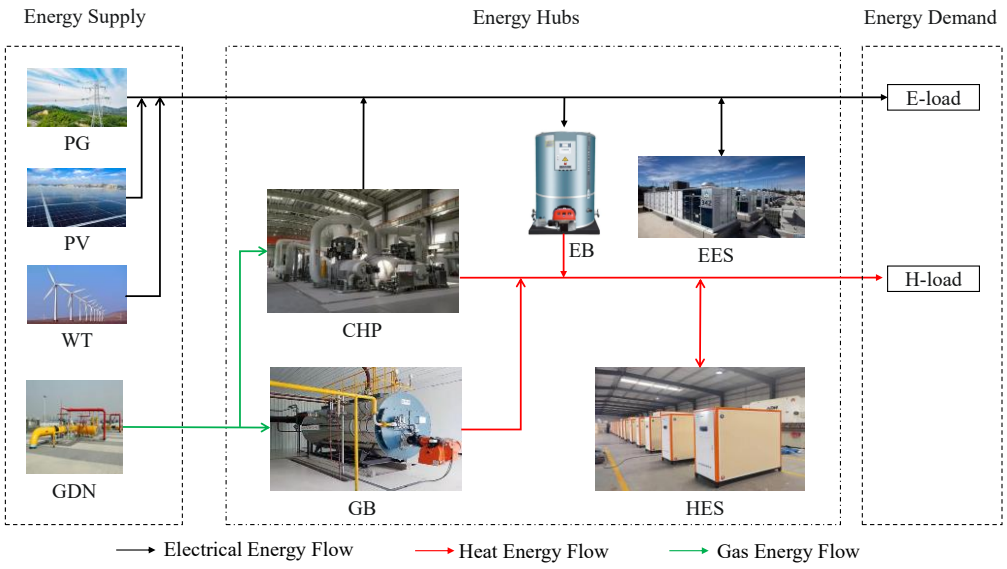

Figure 1. Basic structure of the industrial park EH.

2.2. EH modeling

2.2.1. Principles and modeling of equipment units

1) CHP model

The output power of a GT can be accurately controlled by regulating the consumption of natural gas and the input of compressed air. The electrical output power of the GT can be expressed as:

$$P_t^{CHP,e}t = \eta_e H_L G_t^{CHP,g} \tag{1}$$

where $P_t^{CHP,e}$ represents the electrical power supplied by the CHP unit during a specific time period, η_e denotes the power generation efficiency of the GT, H_L is the lower heating value of natural gas (typically set to 9.7 kW·h/m³), and $G_t^{CHP,g}$ represents the gas consumption of the GT during the considered time period.

Waste heat boilers play a crucial role in increasing the energy utilization efficiency. The recovered thermal power can be expressed as:

$$P_t^{CHP,h} = P_t^{CHP,e}\eta_h\left(1-\eta_e\right)/\eta_e \tag{2}$$

where $P_t^{CHP,h}$ denotes the heat supply power of the CHP unit during the considered time period and η_h represents the efficiency of waste heat recovery.

2) GB model

A gas-fired boiler generates thermal energy by consuming natural gas, which serves as a supplementary heat source for cogeneration units. The relationship between its thermal energy and natural gas consumption can be expressed as:

$$H_t^{GB}t = \eta_{GB,h} H_L G_t^{GB,g} \tag{3}$$

where H_t^{GB} represents the heat supply power of GB during a specific time period, $\eta_{GB,h}$ denotes the heating efficiency of GB, and $G_t^{GB,g}$ represents the gas consumption of GB during the time period.

3) EB model

The mathematical model of the EB can be expressed as:

$$Q_t^{EB} = \eta_{ah} P_t^{EB} \tag{4}$$

where Q_t^{EB} represents the heat generation power of the Electric Boiler (EB) device during a specific time period, η_{ah} represents the efficiency of converting electrical energy to thermal energy for the EB device, and P_t^{EB} represents the electrical power of the EB device during a specific time period.

4) ES model

In the developed EH, the ES devices include electrical and thermal storage components. Their mathematical models can be expressed as:

$$W_{t+1}^{j,i} = \left(1-\sigma^{j,i}\right) W_t^{j,i} + \left(\eta_c^{j,i} P_{t,c}^{j,i} - \frac{P_{t,d}^{j,i}}{\eta_d^{j,i}}\right) \Delta t \tag{5}$$

where j denotes the energy equipment type, i represents the energy type, W_{t+1} and W_t represent the capacities of the ES device at times $t+1$ and t, respectively, σ is the self-discharge coefficient, η_c and η_d are the charging and discharging efficiencies of the ES device, respectively, $P_{t,c}$ and $P_{t,d}$ are the charging and discharging powers of the ES device at time t, respectively, and Δt denotes the time interval.

2.2.2. Energy coupling model

Many devices, including energy conversion and energy storage devices, are used to develop a matrix model. Considering the multi-energy system presented in this study as an example, the following model can be established [25–28]:

$$\begin{bmatrix} L_{e,t} \\ L_{h,t} \end{bmatrix} = \begin{bmatrix} P_{E,t}^{in} \\ 0 \end{bmatrix} - \begin{bmatrix} 1 & -\eta_e^{CHP} & 0 \\ -\eta_{ah} & -\eta_h^{CHP} & -\eta_h^{GB} \end{bmatrix} \begin{bmatrix} P_t^{EB} \\ P_t^{CHP,g} \\ P_t^{GB,g} \end{bmatrix} + \begin{bmatrix} P_{se,t} \\ P_{sh,t} \end{bmatrix} \tag{6}$$

where $L_{e,t}$ and $L_{h,t}$ denote the electrical and thermal load demands of the user during time period t, respectively, η_e^{CHP}, η_h^{CHP}, η_e^{GB}, and η_{ah} represent the energy conversion efficiencies for the CHP electricity, CHP heat, GB, and EB, respectively, and $P_{E,t}^{in}$ is the electrical power input at the EH during time period t, P_t^{EB}, $P_t^{CHP,g}$, and $P_t^{GB,g}$ represent the power consumption of EB, the gas consumption rate of CHP, and the gas consumption rate of GB during time period t, respectively, $P_{se,t}$ and $P_{sh,t}$ represent the power of the electrical and thermal energy storage devices during time period t, respectively.

The electric power $P_{E,t}^{in}$ and gas power $P_{G,t}^{in}$ at the EH input during time period t is given by:

$$P_{E,t}^{in} = P_t^{grid} + P_t^{wind} + P_t^{pv} \tag{7}$$

where P_t^{ex} represents the electrical power purchased by the EH from the grid during the considered time period.

2.3. IES model considering IDR

In the IES, loads are represented by different forms of energy, including electricity, heat, and gas. We model the IDR for multiple load types based on the load analysis methods used in power systems. Based on the flexibility and interactivity of the loads, they can be divided into two parts: Rigid loads (i.e., base load type loads) and flexible loads. In the IES, the flexible loads can be also divided into two forms: Energy shifting and energy substitution [28–30].

2.3.1. IDR modeling

1) Base load

The base load, also known as rigid load, has low flexibility and limited ability to interact with the system. In the aluminum electrolysis IES, this load type typically includes electrical loads for maintenance workshops in aluminum production, heat for the production process, essential electricity, heat, and gas load demands for user facilities.

2) Load transfer type

To perform peak shaving and valley filling and enhance renewable energy consumption, we categorize electrolytic cell loads' participation in DR as transferable loads. Transferable loads should not affect the total system load demand over a scheduling period, meaning the sum of incoming and outgoing loads should be zero. Additionally, there is an upper limit for load transfer, and only one type of load (either outgoing or incoming) can exist at a time. The constraints can be expressed as:

$$\begin{cases} \sum_{t=1}^{T}\left(L_{tr,t,K}^{out}-L_{tr,t,K}^{in}\right)=0 \\ 0\le L_{tr,t,K}^{out}\le L_{tr,t,K}^{out,\max} \\ 0\le L_{tr,t,K}^{in}\le L_{tr,t,K}^{in,\max} \end{cases} \tag{8}$$

where $K\in\{E,H\}$ represents the electricity and heat load types, respectively, $L_{tr,t,K}^{out}$ and $L_{tr,t,K}^{in}$ represent the load transfer out and transfer in quantities during period t (at least one of them should be null within the same period), respectively, and $L_{tr,t,K}^{out,max}$ and $L_{tr,t,K}^{in,max}$ represent the maximum transfer out and transfer in quantities during period t, respectively.

3) Energy substitution load

Energy substitution is the process of leveraging the coupling relationships between multiple energy sources to meet the same load demand with different energy supplies, guided by different energy prices. This substitution relationship enables us to interchange multiple energy sources within the EH. A detailed mathematical expression can be provided by the coupling matrix, which is given by:

$$\begin{cases} \sum_{t=1}^{T}\left(L_{re,t,K}^{out}-L_{re,t,K}^{in}\right)=0 \\ 0\le L_{re,t,K}^{out}\le L_{re,t,K}^{out,\max} \\ 0\le L_{re,t,K}^{in}\le L_{re,t,K}^{in,\max} \end{cases} \tag{9}$$

where $L_{re,t,K}^{out}$ and $L_{re,t,K}^{in}$ represent the load substitution out and substitution in quantities during period t (at least one of them should be null within the same period), respectively, and $L_{re,t,K}^{out,max}$ and $L_{re,t,K}^{in,max}$ represent the maximum substitution out and substitution in quantities during period t, respectively.

2.3.2. Energy coupling model considering IDR

Based on the energy coupling model presented in Eq (9), the integration of IDR can be expressed as:

$$\begin{bmatrix} L_{e,t}+\Delta L_{e,t} \\ L_{h,t}+\Delta L_{h,t} \end{bmatrix}=\begin{bmatrix} P_{E,t}^{in} \\ 0 \end{bmatrix}-\begin{bmatrix} 1 & -\eta_e^{CHP} & 0 \\ -\eta_{ah} & -\eta_h^{CHP} & -\eta_h^{GB} \end{bmatrix}\begin{bmatrix} P_t^{EB} \\ P_t^{CHP,g} \\ P_t^{GB,g} \end{bmatrix}+\begin{bmatrix} P_{se,t} \\ P_{sh,t} \end{bmatrix} \tag{10}$$

where $\Delta L_{e,t}$ and $\Delta L_{h,t}$ represent the demand response quantities of electrical and thermal load powers for the user during time period t, respectively.

3. Economic model and solution method of IES

3.1. Objective function

In this study, the total operating (TO) cost of IES considers the purchased gas (PG) cost C_{FU}, purchased electricity (PE) cost C_{EX}, equipment maintenance (EM) cost C_{ME}, and wind and photovoltaic power abandonment penalty (WPPAP) cost C_{DG}. The objective function is then given by:

$$\min C = C_{FU} + C_{EX} + C_{ME} + C_{DG} \tag{11}$$

1) PG cost

$$C_{FU} = \sum_{t=1}^{T} \alpha(t) P_{g,buy}(t) \tag{12}$$

where $\alpha(t)$ represents the natural gas price during time period t, and $P_{g,buy}(t)$ represents the gas power purchased from GG during time period t.

2) PE cost

$$C_{EX} = \sum_{t=1}^{T} \beta(t) P_{ex}(t) \tag{13}$$

where $\beta(t)$ represents the Electricity Price (EP) during time period t, and $P_{ex}(t)$ represents the electricity power purchased from PG during time period t.

3) EM cost

$$C_{ME} = \sum_{t=1}^{T}\sum_{i=1}^{N_M} C_{mi}\left|P_i(t)\right| \tag{14}$$

where C_{mi} and $P_i(t)$ represent the unit maintenance cost and output power of equipment i during time period t, respectively.

4) WPPAP cost

$$C_{DG} = \delta_{DG}\sum_{t=1}^{T}(P_{WT}^{cut}(t) + P_{PV}^{cut}(t)) \tag{15}$$

where δ_{DG} represents the unit penalty cost of wind and photovoltaic power abandonment, and $P_{WT}^{cut}(t)$ and $P_{PV}^{cut}(t)$ represent the wind and photovoltaic power abandonment during time period t, respectively.

3.2. Constraints

The IES satisfies operation constraints of each equipment and energy balance constraints.

3.2.1. Operation constraints of each equipment

1) Wind power output constraint

$$0 \le P_{WT}(t) \le P_{WT}^{\max} \tag{16}$$

where $P_{WT}(t)$ represents the wind power during time period t, and $P_{WT}^{max}(t)$ represents the upper limit of the wind power output.

2) Photovoltaic power output constraint

$$0 \le P_{PV}(t) \le P_{PV}^{\max} \tag{17}$$

where $P_{PV}(t)$ represents the photovoltaic power during time period t, and $P_{PV}^{max}(t)$ represents the upper limit of the photovoltaic power output.

3) CHP operation constraint

$$\begin{cases} P_{CHP,e}^{\min} \le P_{CHP,e}(t) \le P_{CHP,e}^{\max} \\ P_{CHP}^{down} \le P_{CHP,e}(t) - P_{CHP,e}(t-1) \le P_{CHP}^{up} \end{cases} \tag{18}$$

where $P_{CHP,e}^{\min}$ and $P_{CHP,e}^{\max}$ represent the lower and upper limits of the CHP power, respectively, and P_{CHP}^{down} and P_{CHP}^{up} represent the lower and upper limits of the climb rate of the CHP, respectively.

4) GB operation constraint

$$\begin{cases} H_{GB}^{\min} \le H_{GB}(t) \le H_{GB}^{\max} \\ H_{GB}^{down} \le H_{GB}(t) - H_{GB}(t-1) \le H_{GB}^{up} \end{cases} \tag{19}$$

where H_{GB}^{min} and H_{GB}^{max} represent the lower and upper limits of the GB power, respectively, and $H_{GB}^{down}(t)$ and $H_{GB}^{up}(t)$ represent the lower and upper limits of the climb rate of the GB, respectively.

5) EB operation constraint

$$\begin{cases} Q_{EB}^{\min} \le Q_{EB}(t) \le Q_{EB}^{\max} \\ Q_{EB}^{down} \le Q_{EB}(t) - Q_{EB}(t-1) \le Q_{EB}^{up} \end{cases} \tag{20}$$

where Q_{EB}^{min} and Q_{EB}^{max} represent the lower and upper limits of the EB power, respectively, and $Q_{EB}^{down}(t)$ and $Q_{EB}^{up}(t)$ represent the lower and upper limits of the climb rate of the EB, respectively.

6) ES operation constraint

$$\begin{cases} S_i^{\min} W_i \le W_i(t) \le S_i^{\max} W_i \\ 0 \le P_{i,c}(t) \le x_{i,c}(t) P_{i,c}^{\max} \\ 0 \le P_{i,d}(t) \le x_{i,d}(t) P_{i,d}^{\max} \\ x_{i,c}(t) + x_{i,d}(t) = 1 \\ W_i(0) = W_i(T) \end{cases} \tag{21}$$

where $S_{\mathrm{i}}^{\min}$ and $S_{\mathrm{i}}^{\max}$ represent the lower and upper states of the charge value of ES equipment i, respectively, $P_{i,c}^{\max}$ and $P_{i,d}^{\max}$ represent the upper limits of the charge and discharge powers, respectively, $x_{i,c}$ and $x_{i,d}$ are binary variables representing the current operational state of ES equipment i, and T represents the dispatch cycle.

3.2.2. Energy balance constraint

1) Electricity power balance constraint

$$P_{WT}(t) + P_{PV}(t) + P_{ex}(t) + P_{CHP,e}(t) + P_{EES,d}(t) = L_e(t) + P_{EB}(t) + P_{EES,C}(t) \tag{22}$$

2) Heat power balance constraint

$$P_{CHP,h}(t) + H_{GB}(t) + P_{HES,d}(t) + Q_{EB}(t) = L_h(t) + P_{HES,c}(t) \tag{23}$$

3.3. Solution method

The objective function established in this study belongs to the mixed integer nonlinear programming problem. The standard form of the problem can be formulated as [31,32]:

$$\min F(x)$$
$$s.t. \begin{cases} h_k(x) = 0 & k = 1, 2, \cdots, m \\ g_l(x) \le 0 & l = 1, 2, \cdots, n \\ I \cdot x_{\min} \le x \le I \cdot x_{\max} \\ I \in \{0, 1\} \end{cases} \tag{24}$$

where x represents the output of all the types of power sources (ES, purchased electricity power, and purchased gas power), $h_k(x)$ and $g_l(x)$ are equal and unequal constraints corresponding to the power balance constraints and the equipment operation power constraints, respectively, m and n represent the number of equal and unequal constraints, respectively, x_{min} and x_{max} represent the upper and lower limits of the equipment operation power, respectively, and I represents the state variable.

We transform the aforementioned problem into a mixed integer linear programming problem, which can be directly solved using CPLEX.

4. Experiments and analysis

4.1. Parameter settings

An industrial park in the south of China is considered the research object. This industrial park includes WT, PV, CHP, EB, GB, EES, and HES. The typically predicted outputs of WT, PV, electrical and heat loads are shown in Figure 2. The dispatch periods are of 24 h, each with a unit time of 1 h. The parameters related to each equipment of the IES are shown in Table 1. The time-of-use EP and gas price are shown in Table 2. The parameters of the ES system are shown in Table 3 [33].

We minimize the TO cost of IES by efficiently processing WT, PV, loads, and market prices data.

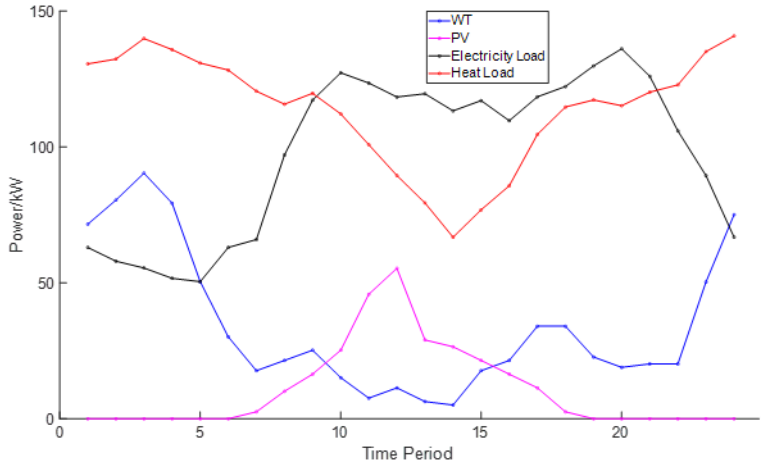

Figure 2. Predicted output of renewable energy and loads.

Table 1. Operation parameters of the IES.

Type	P_{min}/kW	P_{max}/kW	R_{down}/kW	R_{up}/kW	Cm/ (CNY/kW)
GT	0	65	−5	10	0.0250
EB	0	50	−3	5	0.0160
WT	0	100	—	—	0.0196
PV	0	60	—	—	0.0235
GB	0	200	−10	10	0.0160

Table 2. Time-of-use EP and natural gas price.

Time period	Electricity price (CNY/(kW·h))	Gas price (CNY/(kW·h))
1–7，23–24	0.17	0.35
8–11，15–18	0.49	0.35
12–14，19–22	0.83	0.35

Table 3. Operating parameters of the ES equipment.

Type	Charge/discharge rate	self-loss rate	$P_{max,c}$/kW	$P_{max,c}$/ kW	S_{max}	S_{min}	W_0/ (kW·h)	W/ (kW·h)	Gas price/ (CNY/kW)
EES	0.17	0.001	37.5	37.5	0.8	0.2	30	150	0.35
HES	0.49	0.01	25	25	0.8	0.1	20	100	0.35

To optimize the IES operation, the following seven scenarios are adopted for comparative analysis: Scenarios 1, 2, and 3 are energy conversion parallel comparisons, Scenarios 4, 5, and 6 are industrial parks considering multiple energy conversion equipment, and Scenario 7 further takes the IDR into consideration. In summary:

Scenario 1: EB only on the EH side.

Scenario 2: GB only on the EH side.

Scenario 3: CHP only on the EH side.

Scenario 4: CHP is introduced based on Scenario 2.

Scenario 5: EB is introduced based on Scenario 4.

Scenario 6: ES equipment is introduced based on Scenario 5.

Scenario 7: IDR is introduced based on Scenario 6.

The dispatch results of the aforementioned 7 scenarios are shown in Table 4. A detailed analysis is conducted in Section 4.2.

Table 4. Dispatch results of the 7 scenarios.

Scenarios	TO cost/CNY	PG cost/CNY	PE cost/CNY	EM cost/CNY	WPPAP cos/CNY
1	2214.67	0	2147.59	67.08	0
2	1748.44	829.16	842.99	66.11	10.18
3	1525.26	1373.90	72.18	69.00	10.18
4	1548.61	1176.29	259.89	77.99	34.44
5	1463.03	1072.98	301.40	77.68	10.97
6	1351.60	1068.47	200.71	77.67	4.75
7	1276.45	1102.79	90.45	79.13	4.08

4.2. Comparative analysis of energy conversion equipment parallel scenarios

Scenarios 1, 2, and 3 are used to compare and analyze the impacts of the single energy conversion equipment on the IES operation. It can be seen from Table 4 that the TO cost of Scenario 1 is the highest, that of Scenario 2 is reduced by 21.05% compared with Scenario 1, and that of Scenario 3 is reduced by 12.76% compared with Scenario 2. This indicates that different single energy conversion equipment has a significant impact on the operating cost of the integrated energy system, and the rational choice of equipment can effectively reduce the operating cost of the system. The dispatch results of electricity and heat loads in Scenarios 1, 2, and 3 are shown in Figures 3 and 4.

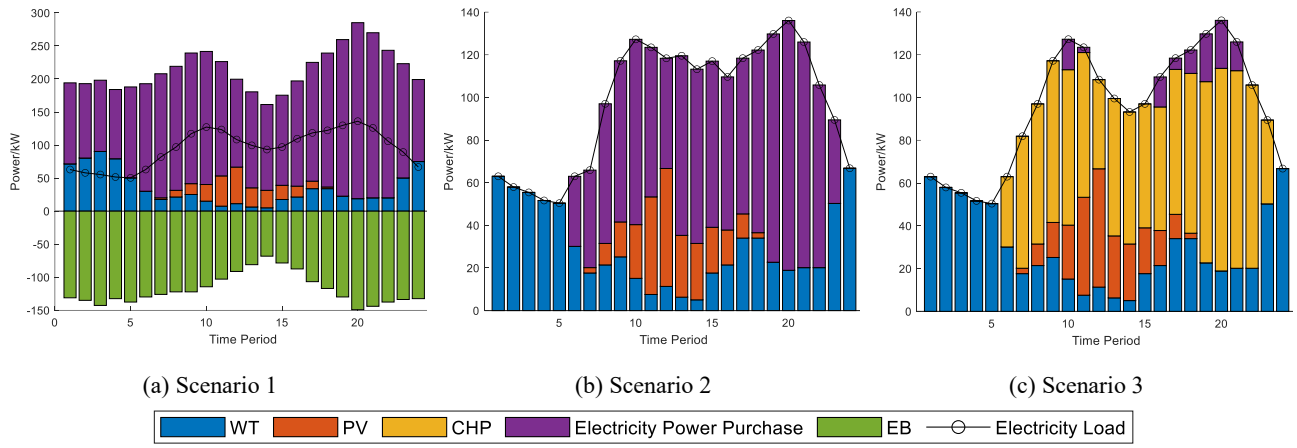

Figure 3. Electricity power balance diagrams in Scenarios 1, 2, and 3.

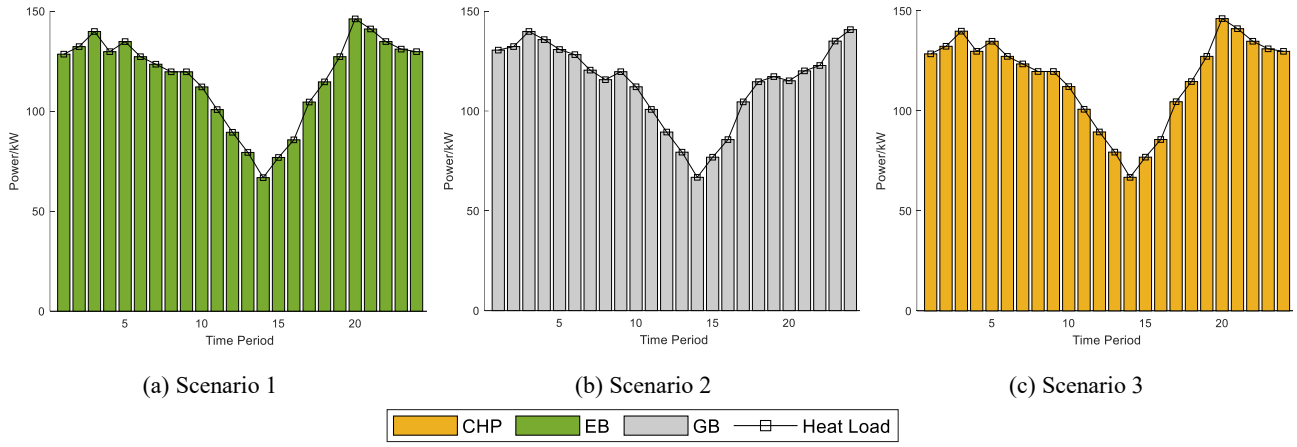

Figure 4. Heat power balance diagrams in Scenarios 1, 2, and 3.

CHP is the energy conversion equipment on the EH side. It consumes natural gas and can generate electricity and heat loads. Therefore, it can generate electricity with lower-priced natural gas during peak electricity prices, which enables us to minimize the TO cost. GB is the energy conversion equipment on the EH side in Scenario 2. It consumes natural gas to generate only heat load. The shortage of electricity load should be purchased from the PG, which results in increasing the TO cost.

EB is the energy conversion equipment on the EH side. It consumes electricity to produce heat. In this Scenario, there is no consumption of natural gas, which yields the highest TO cost.

4.3. Analysis of energy conversion equipment configuration

The TO cost in Scenario 4 is reduced by 11.43% compared with that in Scenario 2 after introducing CHP. The TO cost in Scenario 5 is reduced by 5.53% compared with that of Scenario 4 after introducing EB. In addition, after introducing the ES equipment in Scenario 6, the TO cost is reduced by 7.62% compared with that of Scenario 5. This indicates that the rational configuration of equipment such as CHP, EB and ES can further optimize the operating economy of IES, which has a positive and effective effect on reducing the TO cost. The dispatch results of electricity and heat loads in Scenarios 4, 5, and 6 are shown in Figures 5 and 6, respectively.

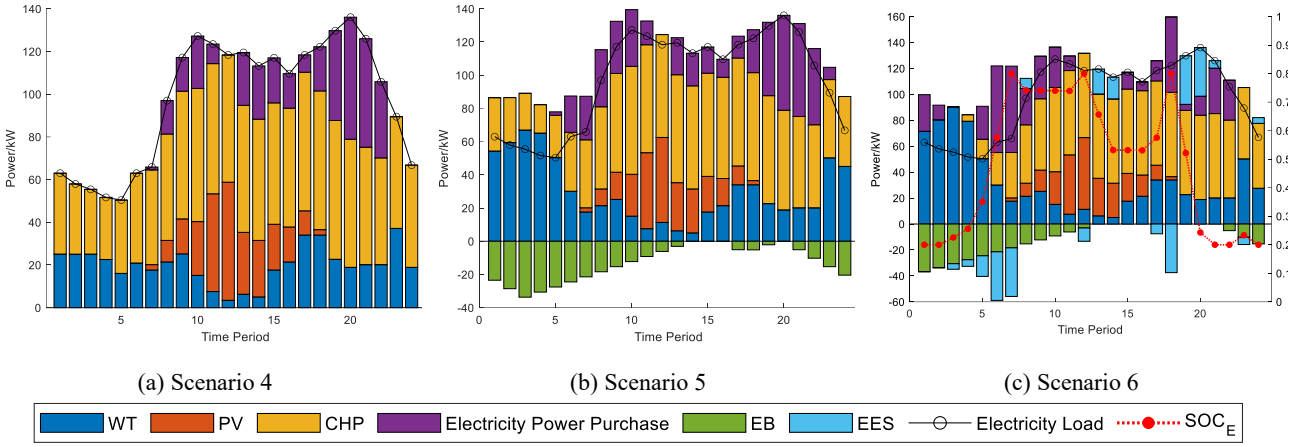

Figure 5. Electricity power balance diagrams in Scenarios 4, 5, and 6.

It can be seen from Figure 5 that Scenarios 4, 5, and 6 prioritize the use of wind and photovoltaic power. When CHP is introduced based on Scenario 2, the amount of wind and photovoltaic power curtailment in Scenario 4 increases compared to Scenario 2. This is due to the fact that, when taking the operation constraints of the CHP into consideration, it starts to operate during the low EP periods of 1–7 to ensure ta maximum power in the peak periods of electricity consumption. Although the PG cost is increased, the savings in the PE cost are higher, which results in reducing the TO cost. After introducing EB based on Scenario 4, the amount of wind and photovoltaic abandonment in Scenario 5 is reduced. This is due to the fact that the excess of wind and photovoltaic power can be converted to heat energy through EB to meet the demand of heat load. Consequently, the outputs of CHP and GB are mitigated, the PG cost is reduced, the PE cost is slightly increased, and the TO cost is reduced. After introducing the EES in Scenario 6, the excess of energy is saved in EES in the case of high wind and photovoltaic outputs. Therefore, the wind and photovoltaic abandonment is further reduced, and electricity power is purchased from the PG for storage during the low EP periods 1–7. Moreover, electricity power is discharged during the peak electricity consumption periods, with lower PE and TO costs.

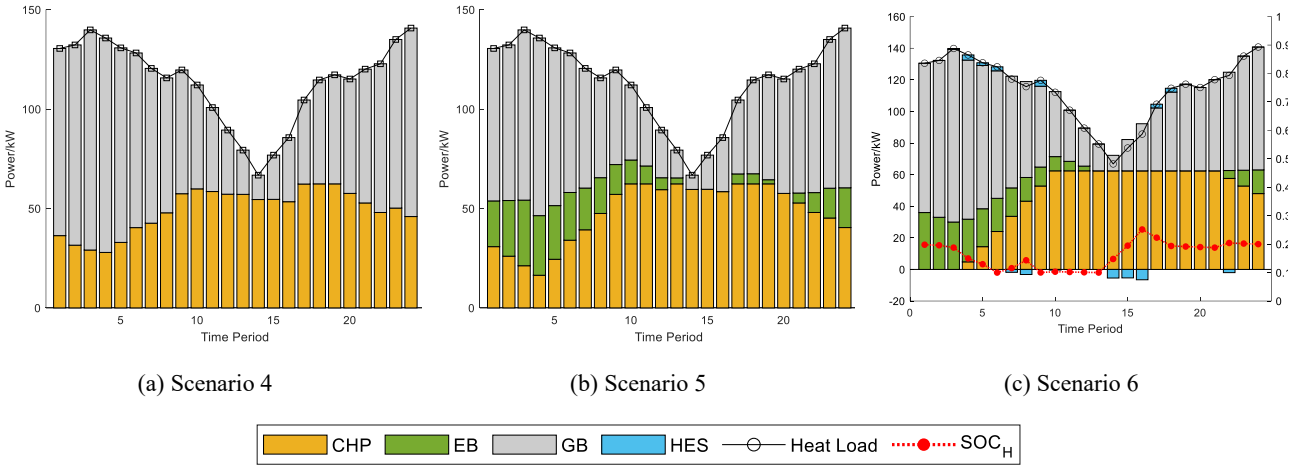

(a) Scenario 4 (b) Scenario 5 (c) Scenario 6

Figure 6. Heat power balance diagrams in Scenarios 4, 5, and 6.

It can be seen from Figure 6 that Scenarios 4, 5, and 6 meet the demand of their heat load by the more energy-efficient GB during the low EP periods 1–7 and 23–24. This is due to the fact that during these periods, the CHP heating reduces the IES revenue. Moreover, during periods 8–22, CHP should produce more electricity power for the system to gain a higher revenue, and therefore the CHP heating is increased. The shortage is replenished by the rest of the heating equipment in the IES. The difference is that in Scenario 4, the heat load shortage is supplemented by CHP during the low EP periods 1–7 and 23–24, and by GB during periods 8–22. In Scenario 5, the heat load shortage is supplemented by CHP and EB during the low EP periods 1–7 and 23–24, and most of the heat load shortage is supplemented by GB during periods 8–22, yielding less EB output. Finally, in Scenario 6, the heat load shortage is supplemented by GB, EB, and HES during the low EP periods 1–7 and 23–24, the CHP heating increases, and the excess heat load is stored in the HES.

4.4. Analysis of the IDR impact

4.4.1. Analysis of operational optimization results

Scenarios 6 and 7 are used to analyze the impact of the IDR on the IES operation. It can be observed from Table 4 that after considering IDR in Scenario 7, the PE cost is reduced compared with that in Scenario 6. Although the PG cost is increased, the saved PE cost is higher. Therefore, the TO cost is reduced by 5.56%, and the amount of wind and photovoltaic power abandonment is reduced, which improves the economy and increases the environmental performance of the system. This indicates that IDR can effectively optimize the operation of IES and achieve a win-win situation in terms of economic and environmental benefits. The dispatch results of electricity and heat loads of Scenario 7 are shown in Figures 7 and 8, respectively.

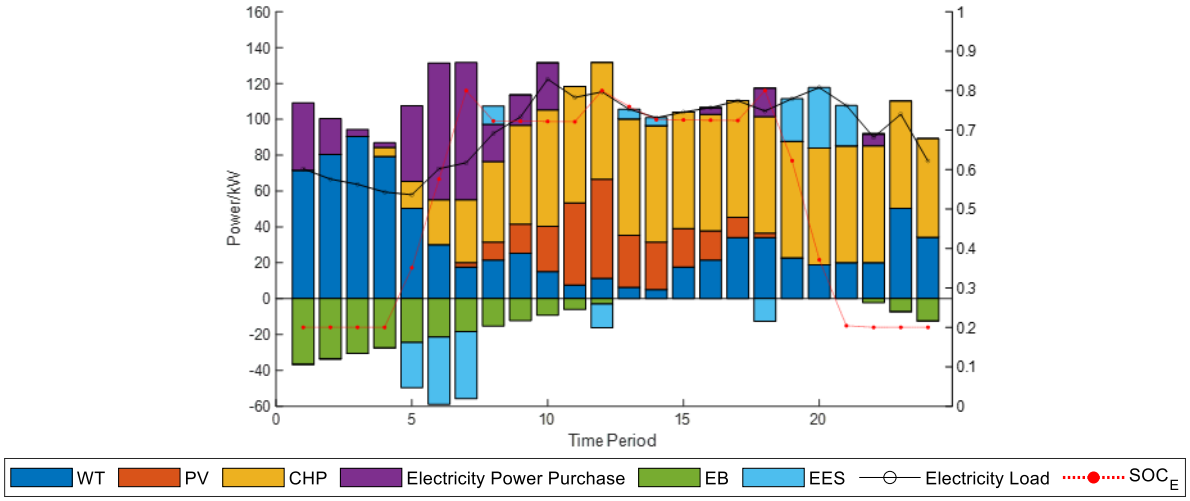

Figure 7. Electricity power balance diagrams in Scenario 7.

It can be seen from Figure 7 that Scenario 7 also prioritizes the use of wind and photovoltaic power. After considering IDR in Scenario 7, compared with Scenario 6, the electricity load curve increases during the low EP periods 1–7 and 23–24, and the IES increases the electricity power purchase from the PG. During periods 8–22, the electricity load curve decreases in Scenario 7. In addition, since the PE cost is higher than the CHP operation cost, the system increases the use of CHP and reduces the purchase of electricity power from the PG. Therefore, the PE cost is reduced.

Furthermore, it can be observed from Figure 8 that Scenario 7 also prioritizes the use of more efficient GB for heat supply during the peak heat periods 1–7 and 23–24, while the shortage is supplemented by CHP, EB, and HES. After considering IDR in Scenario 7, the heat load curve and the use of EB are reduced during the peak heat periods. When increasing the heat load demand with the more energy-efficient GB during the low heat periods 8–22, the IES economy is improved.

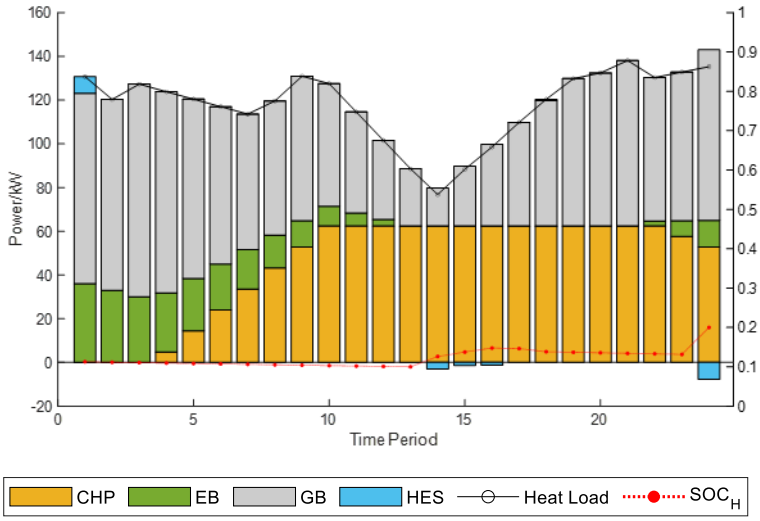

Figure 8. Heat power balance diagrams in Scenario 7.

4.4.2. Analysis of the fluctuation of load curves

Scenarios 6 and 7 are used to analyze the impact of the IDR on the load fluctuation. Figure 9 shows the curve diagrams of electricity and heat loads before and after considering IDR. It can be seen that the users use less electricity and more heat at night, while they use more electricity and less heat during the day. After considering IDR, the users reduce the load peak and valley differences according to the EP signal. During periods 1–7 and 23–24, the users shift their electricity consumption from the peak hours to these periods in order to increase the consumption of renewable energy. Moreover, part of the heat load is replaced by the electricity load, and the curve of the latter is elevated. At these periods, the demand of heat load is high, and thus its shifts and load curve are reduced. During periods 8–22, due to the higher electricity prices, users use more heat load to meet their energy demand, part of the electric load is replaced by the heat load, and the electric load curve is lowered. After considering IDR, the peak and valley difference of the electric load curve is decreased by 24.78%, and the peak and valley difference of the heat load curve is decreased by 17.11%. This enables us to achieve the effect of cutting peaks and filling valleys, effectively smoothing the energy consumption curves of the user and reducing the pressure on the PG energy supply.

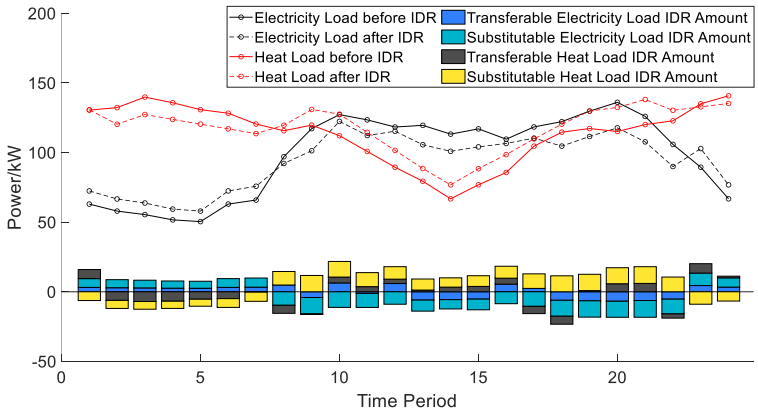

Figure 9. Load curves before and after IDR.

5. Conclusions

We propose a dispatch model to optimize the IES operation. This model compares the energy conversion equipment parallel scenarios, energy conversion equipment configuration methods, and IDR. An EH model, which takes multiple energy sources into consideration, is first developed. In addition, an IDR model, which takes the horizontal shift of loads and vertical complementary substitution into consideration, is developed. An optimal dispatch model is then developed to minimize the sum of purchased gas cost, purchase electricity cost, equipment maintenance cost, and wind and photovoltaic power abandonment penalty cost. Finally, the CPLEX is applied to solve the underlying problem, and the optimal dispatch strategy for IES is established.

The experimental results show that, compared with energy conversion equipment parallel scenarios, the CHP, which can simultaneously generate electricity and heat loads, yields the lowest total operating cost. Therefore, during peak EP periods, it can generate electricity by natural gas with lower price. The TO cost of separately configuring CHP has been reduced by 21.05% and 12.76%

compared to separately configuring EB and GB, respectively. In the configuration of the energy conversion equipment, the economy of IES and the renewable energy consumption are improved by configuring various energy conversion equipment within the IES. After configuring various energy equipment, the TO cost is reduced by 11.39% compared to only configuring CHP. The IES economy can be further improved by considering the IDR. The total operating cost is reduced by 5.56%, while the electricity and heat load curves of the users are reduced by 24.78% and 17.11%, respectively. This enables us to achieve the purpose of cutting peaks and filling valleys.

This study also has many limitations. In future work, we aim to optimize the equipment capacity configuration under the impact of wind and photovoltaic uncertainties in order to achieve the best economy and highest grid stability.

Use of AI tools declaration

The authors declare that no Artificial Intelligence (AI) tools have been used in the creation or revision of this article. The content is entirely the original work of the authors.

Acknowledgments

This work is supported by the Science and Technology Project of China Southern Power Grid Co., Ltd (ZBKJXM20232275).

Conflict of interest

The authors declare no conflicts of interest.

Author contributions

Conceptualization, Xin Jin and Tingzhe Pan; methodology, Xin Jin and Tingzhe Pan; software, Ruoli Tang; validation, Xin Li and Tingzhe Pan; formal analysis, Tingzhe Pan; investigation, Zongyi Wang; resources, Ruoli Tang; data curation, Ruoli Tang; writing—original draft preparation, Xin Jin and Tingzhe Pan; writing—review and editing, Zongyi Wang; visualization, Chao Jiang and Rui Zhang; supervision, Chao Jiang; funding acquisition, Tingzhe Pan. All authors have read and agreed to the published version of the manuscript.

References

1. Li YZ, Wang D, Jia HJ, et al. (2023) Research on the diversity modeling and typical applicability of energy hubs in integrated energy systems. *Integr Intell Energy* 45: 22–29. https://doi.org/10.3969/j.issn.2097-0706.2023.07.003
2. Gao X, Lin H, Jing D, et al. (2025) A novel framework for optimal design of solar-powered integrated energy system considering long timescale characteristics. *Energy* 325: 136137. https://doi.org/10.1016/j.energy.2025.136137

3. Ao X, Zhang J, Yan R, et al. (2025) More flexibility and waste heat recovery of a combined heat and power system for renewable consumption and higher efficiency. *Energy* 315: 134392. https://doi.org/10.1016/j.energy.2025.134392
4. Dai ZK, Zeng G, Shi KJ, et al. (2023) A multi-energy hub load-source coordination optimization method considering the benefits of energy consumption. *Sci, Technol Eng* 23: 14603–14608. https://doi.org/10.12404/j.issn.1671-1815.2211286.
5. Li HW, Jing HJ, Wu L, et al. (2023) Optimization operation of electric thermal grids based on the variable energy efficiency of energy hubs. *J Zhengzhou Univ* 44: 76–83. https://doi.org/10.13705/j.issn.1671-6833.2023.04.015.
6. Wang L, Xie Q, Sun L (2023) Optimization operation of energy hubs considering energy storage systems. *J Zhengzhou Univ* 51: 1–6. https://doi.org/10.16109/j.cnki.jldl.2023.06.012
7. Wang MY, Wang RQ, Liu JY, et al. (2022) Operation optimization for park with integrated energy system based on integrated demand response. *Energy Rep* 8: 249–259. https://doi.org/10.1016/j.egyr.2022.05.060
8. Guo ZH, Zhang R, Wang L, et al. (2021) Optimal operation of regional integrated energy system considering demand response. *Appl Therm Eng* 191: 18. https://doi.org/10.1016/j.applthermaleng.2021.116860
9. Li P, Zhang F, Ma XY, et al. (2021) Multi-time scale economic optimization dispatch of the park integrated energy system. *Front Energy Res* 9: 12. https://doi.org/10.3389/fenrg.2021.743619
10. Xu CS, Dong SF, Zhang SP, et al. (2021) Centralized-distributed integrated demand response method for industrial parks. *Power Syst Technol* 45: 489–497. https://doi.org/10.13335/j.1000-3673.pst.2020.0945
11. Chong Z, Yang L, Jiang Y, et al. (2024) Hybrid-timescale optimal dispatch strategy for electricity and heat integrated energy system considering integrated demand response. *Renewable Energy* 232: 121123. https://doi.org/10.1016/j.renene.2024.121123
12. Duan J, Tian Q, Liu F, et al. (2024) Optimal scheduling strategy with integrated demand response based on stepped incentive mechanism for integrated electricity-gas energy system. *Energy* 313: 133689. https://doi.org/10.1016/j.energy.2024.133689
13. Nourizadeh H, Nazar MS (2024) Customer-oriented scheduling of active distribution system considering integrated demand response programs and multi-carrier energy hubs. *J Clean Prod* 447: 141308. https://doi.org/10.1016/j.jclepro.2024.141308
14. Wang M, Zheng JH, Li ZG, et al. (2022) Multi-attribute decision analysis for optimal design of park-level integrated energy systems based on load characteristics. *Energy* 254: 23. https://doi.org/10.1016/j.energy.2022.124379
15. Liu ZF, Zhao SX, Luo XF, et al. (2025) Two-layer energy dispatching and collaborative optimization of regional integrated energy system considering stakeholders game and flexible load management. *Appl Energy* 379: 124918. https://doi.org/10.1016/j.apenergy.2024.124918
16. Liu Y, Zheng R, Shen R, et al. (2025) Research on capacity configuration optimization of integrated energy system by integrating energy hub and response surface methodology. *Energy* 136348. https://doi.org/10.1016/j.energy.2025.136348
17. Li S, Zhu J, Dong H, et al. (2024) Multi-time-scale energy management of renewable microgrids considering grid-friendly interaction. *Appl Energy* 367: 123428. https://doi.org/10.1016/j.apenergy.2024.123428

18. Fan J, Yan R, He Y, et al. (2025) Stochastic optimization of combined energy and computation task scheduling strategies of hybrid system with multi-energy storage system and data center. *Renewable Energy* 242: 122466. https://doi.org/10.1016/j.renene.2025.122466
19. Zhao Z, Xu H, Bao G (2025) Study on energy resource-project mode-load demand chain flexibility adaptation of park-level integrated energy systems. *Energy* 320: 135246. https://doi.org/10.1016/j.energy.2025.135246
20. Xie T, Ma K, Zhang G, et al. (2024) Optimal scheduling of multi-regional energy system considering demand response union and shared energy storage. *Energy Strateg Rev* 53: 101413. https://doi.org/10.1016/j.esr.2024.101413
21. Yu J, Chen L, Wang Q, et al. (2024) Towards sustainable regional energy solutions: An optimized operational model for integrated energy systems with price-responsive planning. *Energy* 305: 132278. https://doi.org/10.1016/j.energy.2024.132278
22. Huang A, Bi Q, Dai L (2025) Integrated economic and environmental optimization for industrial consumers: A dual-objective approach with multi-carrier energy systems and fuzzy decision-making. *Energy* 324: 135787. https://doi.org/10.1016/j.energy.2025.135787
23. Jordehi AR, Mansouri SA, Tostado-Véliz M, et al. (2024) Industrial energy hubs with electric, thermal and hydrogen demands for resilience enhancement of mobile storage-integrated power systems. *Int J Hydrogen Energy* 50: 77–91. https://doi.org/10.1016/j.ijhydene.2023.07.205
24. Sepehrzad R, Al-Durra A, Anvari-Moghaddam A, et al. (2025) Short-term and probability scenario-oriented energy management of integrated energy distribution systems with considering energy market interactions and end-user participation. *Energy* 322: 135691. https://doi.org/10.1016/j.energy.2025.135691
25. Zhang XP (2019) Optimal expansion planning of energy hub with multiple energy infrastructures. *South Energy Constr* 6: 6–12. https://doi.org/10.16516/j.gedi.issn2095-8676.2019.04.002
26. Wang R, Cheng S, Xu JY, et al. (2023) Multi-time scale optimal scheduling strategy of energy hub based on master-slave game and hybrid demand response. *Electr Power Autom Equip* 43: 32–40. https://doi.org/10.16081/j.epae.202204055
27. Zhu XP, Yao XY, Fu Q, et al. (2022) Optimized operation mode considering cooperation among energy hubs. *Modern Electric Power* 39: 397–405. https://doi.org/10.19725/j.cnki.1007-2322.2021.0168
28. Song TL (2020) Study on integrated port energy system considering demand response. *South Univ* https://doi.org/10.1016/j.ijepes.2019.105654
29. Wang LM, Liu XM, Li Y, et al. (2024) Low-carbon optimal dispatch of integrated energy system considering demand response under the tiered carbon trading mechanism. *Electr Power Constr* 45: 102–114. https://doi.org/10.12204/j.issn.1000-7229.2024.02.009
30. Chen JP, Hu ZJ, Chen JB, et al. (2021) Optimal dispatch of integrated energy system considering ladder-type carbon trading and flexible double response of supply and demand. *High Voltage Eng* 47: 3094–3106. https://doi.org/10.13336/j.1003-6520.hve.20211094
31. Yang HZ, Li ML, Jiang ZY, et al. (2020) Optimal operation of regional integrated energy system considering demand side electricity heat and natural-gas loads response. *Power Syst Prot Control* 48: 30–37. https://doi.org/10.19783/j.cnki.pspc.190774
32. Chen JP, Hu ZJ, Chen YG, et al. (2021) Thermoelectric optimization of integrated energy system considering ladder-type carbon trading mechanism and electric hydrogen production. *Electr Power Autom Equip* 41: 48–55. https://doi.org/10.16081/j.epae.202109032

33. Li ZM, Zhang F, Liang J, et al. (2015). Optimization on microgrid with combined heat and power system. *Proc CSEE* 35: 3569–3576. https://doi.org/10.13334/j.0258-8013.pcsee.2015.14.011